The Journal of Physiology

Coupling of excitation to Ca^{2+} release is modulated by dysferlin

Valeriy Lukyanenko, Joaquin M. Muriel and Robert J. Bloch

Department of Physiology, University of Maryland School of Medicine, Baltimore, MD, USA

Key points

- Dysferlin, the protein missing in limb girdle muscular dystrophy 2B and Miyoshi myopathy, concentrates in transverse tubules of skeletal muscle, where it stabilizes voltage-induced Ca^{2+} transients against loss after osmotic shock injury (OSI).
- Local expression of dysferlin in dysferlin-null myofibres increases transient amplitude to control levels and protects them from loss after OSI.
- Inhibitors of ryanodine receptors (RyR1) and L-type Ca^{2+} channels protect voltage-induced Ca^{2+} transients from loss; thus both proteins play a role in injury in dysferlin's absence. Effects of Ca^{2+}-free medium and S107, which inhibits SR Ca^{2+} leak, suggest the SR as the primary source of Ca^{2+} responsible for the loss of the Ca^{2+} transient upon injury.
- Ca^{2+} waves were induced by OSI and suppressed by exogenous dysferlin.
- We conclude that dysferlin prevents injury-induced SR Ca^{2+} leak.

Abstract Dysferlin concentrates in the transverse tubules of skeletal muscle and stabilizes Ca^{2+} transients when muscle fibres are subjected to osmotic shock injury (OSI). We show here that voltage-induced Ca^{2+} transients elicited in dysferlin-null A/J myofibres were smaller than control A/WySnJ fibres. Regional expression of Venus-dysferlin chimeras in A/J fibres restored the full amplitude of the Ca^{2+} transients and protected against OSI. We also show that drugs that target ryanodine receptors (RyR1: dantrolene, tetracaine, S107) and L-type Ca^{2+} channels (LTCCs: nifedipine, verapamil, diltiazem) prevented the decrease in Ca^{2+} transients in A/J fibres following OSI. Diltiazem specifically increased transients by ∼20% in uninjured A/J fibres, restoring them to control values. The fact that both RyR1s and LTCCs were involved in OSI-induced damage suggests that damage is mediated by increased Ca^{2+} leak from the sarcoplasmic reticulum (SR) through the RyR1. Congruent with this, injured A/J fibres produced Ca^{2+} sparks and Ca^{2+} waves. S107 (a stabilizer of RyR1–FK506 binding protein coupling that reduces Ca^{2+} leak) or local expression of Venus-dysferlin prevented OSI-induced Ca^{2+} waves. Our data suggest that dysferlin modulates SR Ca^{2+} release in skeletal muscle, and that in its absence OSI causes increased RyR1-mediated Ca^{2+} leak from the SR into the cytoplasm.

(Resubmitted 18 April 2017; accepted after revision 16 May 2017; first published online 1 June 2017)
Corresponding author R. J. Bloch: Department of Physiology, University of Maryland School of Medicine, 580C HSF1, 685 W. Baltimore Street, Baltimore, MD 21201, USA. Email: rbloch@som.umaryland.edu

Abbreviations A/J, dysferlin-null myofibres; A/W, A/WySnJ control myofibres; CICR, Ca^{2+}-induced Ca^{2+}-release; CICT, Ca^{2+}-induced Ca^{2+}-transient; DHPR, dihydropyridine receptor; ECC, excitation–contraction coupling; FDB, flexor digitorum brevis; FKBP, FK506 binding protein; LTCC, L-type Ca^{2+} channel; OSI, osmotic shock injury; RyR1, ryanodine receptor; SOICR, store-overload-induced Ca^{2+} release; SR, sarcoplasmic reticulum; T-tubule, transverse tubule; V-Dysf, N-terminal Venus chimera of wild-type dysferlin.

 DOI: 10.1113/JP274515

Introduction

Excitation–contraction coupling (ECC) in skeletal muscle fibres occurs through direct mechanical coupling between the L-type Ca^{2+} channel (LTCC), located in the membrane of the transverse tubule (T-tubule), and the ryanodine receptor (RyR1), the SR Ca^{2+} release channel located in the terminal cisternal membrane (Rios *et al.* 2015; Bannister, 2016). Defective regulation of Ca^{2+} homeostasis has been considered to underlie many pathologies of skeletal muscle (Burr & Molkentin, 2015), beginning with the demonstration that some mutations in the RyR1 that cause malignant hyperthermia were associated with increased Ca^{2+} leak from the SR lumen into the myoplasm (Tong *et al.* 1999; Dirksen & Avila, 2004; Yang *et al.* 2007). The mechanisms linking the initiation and progression of myopathies and muscular dystrophies to changes in Ca^{2+} homeostasis have not yet been fully elucidated, however. This is especially true for the large class of diseases classified as limb girdle muscular dystrophies (LGMD; reviewed in Nigro & Savarese, 2014; Vissing, 2016). We have been studying diseases of this class caused by mutations in the human *DYSF* gene, which encodes the protein dysferlin.

Dysferlin is a ∼230 kDa integral membrane protein that is missing or mutated in limb girdle muscular dystrophy type 2B, Miyoshi myopathy and distal myopathy with anterior tibial onset (Liu *et al.* 1998; Liewluck *et al.* 2009). Most studies of dysferlin's function have focused on its possible role in the repair of the sarcolemmal membrane (Bansal *et al.* 2003; Bansal & Campbell, 2004; Glover & Brown, 2007; Roche *et al.* 2010; Defour *et al.* 2014; McDade *et al.* 2014; Demonbreun *et al.* 2016) and in membrane trafficking (Glover & Brown, 2007; Hernandez-Deviez *et al.* 2008; Evesson *et al.* 2010; Han *et al.* 2012; Oulhen *et al.* 2014). As dysferlin is also expressed in monocytes (Nagaraju *et al.* 2008), its role in the inflammation associated with dysferlinopathies has also been explored (McNally *et al.* 2000; Rawat *et al.* 2010; Farini *et al.* 2012; Mariano *et al.* 2013; Uaesoontrachoon *et al.* 2013; Roche *et al.* 2015; Yin *et al.* 2015; Urao *et al.* 2016). Our most recent studies suggest that dysferlin's role in mature skeletal muscle is likely to be limited largely to the T-tubules, where it concentrates (Roche *et al.* 2011; Kerr *et al.* 2013, 2014). Given this range of possibilities, it is perhaps not surprising that the pathophysiological events that underlie the degeneration of muscle tissue in dysferlinopathies are still controversial.

As noted above, dysregulation of cytoplasmic Ca^{2+} is a pathological feature common to many muscular dystrophies (Burr & Molkentin, 2015). Mature, dysferlin-null skeletal muscle is more susceptible to injury, which leads to a reduction in the amplitude of the voltage-induced Ca^{2+} transients *in vitro* and a prolonged loss of contractile torque *in vivo* (Roche *et al.* 2008, 2010; Millay *et al.* 2009; Kerr *et al.* 2013). This suggests that Ca^{2+} signalling is also likely to be defective in dysferlinopathies. This idea is supported by the observation that both effects of injury are inhibited by diltiazem (Kerr *et al.* 2013), a benzothiazepine that blocks LTCCs (also referred to as dihydropyridine receptors; DHPRs) in skeletal muscle without inhibiting their mechanochemical coupling to ryanodine receptors (RyR1) (Gonzalez-Serratos *et al.* 1982; Williams, 1990; Böhle, 1992). Based on these observations, we hypothesized that dysferlin's primary function at the T-tubule of mature skeletal muscle is to stabilize the mechanisms underlying voltage-induced Ca^{2+} release at the triad junction (Kerr *et al.* 2013,2014). In the experiments reported here, we show that the expression of dysferlin in A/J myofibres restores the normal amplitude of the voltage-induced Ca^{2+} transient and protects it against loss following injury, consistent with this hypothesis.

We have also proposed that the dysregulation of the Ca^{2+} release mechanism that occurs in dysferlin-null muscle contributes significantly to the pathophysiology seen in dysferlinopathies. Such dysregulation most commonly involves uncoupling the mechanochemical links between the LTCC and the RyR1, which can lead to increases in the cytoplasmic levels of Ca^{2+} via increased release of Ca^{2+} from the lumen of the sarcoplasmic reticulum (SR) through RyR1. The increase in Ca^{2+} leak can be activated by a number of factors, including higher local $[Ca^{2+}]$ within the SR lumen or in the cytoplasm adjacent to the triad junction (Endo, 2009; Lanner *et al.* 2010). If this mechanism contributes to the pathophysiology of dysferlinopathy, then we would expect to observe Ca^{2+} release events in injured dysferlin-null myofibres *in vitro*, including Ca^{2+} waves and Ca^{2+} sparks, which can be suppressed by local expression of dysferlin. Furthermore, injury leading to dysregulation of Ca^{2+} influx should be blocked or ameliorated by drugs that block Ca^{2+} flux through the RyR1 as well as by drugs that, like diltiazem, block Ca^{2+} flux through the DHPR. Our experiments, described below, confirm these predictions in myofibres from the dysferlin-null A/J mouse (Ho *et al.* 2004; Kerr *et al.* 2013). We also report the novel observation that the Ca^{2+} waves induced in A/J muscle fibres by osmotic shock injury (OSI) are suppressed by the local expression of dysferlin, or by S107, an inhibitor of RyR1-mediated Ca^{2+} leak. Our results support the hypothesis that a major role of dysferlin in mature skeletal muscle is to stabilize the mechanochemical coupling of the LTCC and RyR1 that is essential for normal Ca^{2+} release and excitation–contraction coupling (ECC).

Methods

Ethical approval

All animal procedures were in compliance with the *Guide for the Care and Use of Laboratory Animals* (NIH publication No. 85-23, revised 1996). All experimental protocols involving animals were approved by the Institutional Animal Care and Use Committee of the University of Maryland School of Medicine.

Mice

Dysferlin-null (A/J) and control (A/WySnJ, or A/W) mice were obtained either directly from The Jackson Laboratory (Bar Harbor, ME, USA) or from breeding colonies maintained at the University of Maryland, Baltimore. Mice were anaesthetized by inhalation of 2.5% isoflurane vaporized in oxygen and killed by cervical dislocation. All mice used for this study were 12–16 weeks of age.

Plasmid constructs and transfection

mVenus-dysferlin (N-terminal Venus) (Addgene plasmid 29768) (Covian-Nares *et al.* 2010) was provided by The Jain Foundation (www.jain-foundation.org). *In vivo* gene transfer via electroporation into flexor digitorum brevis (FDB) fibres was adapted from published methods (DiFranco *et al.* 2006, 2011), as described (Kerr *et al.* 2013). Venus-dysferlin (V-Dysf) was visualized in cultured myofibres (see below) with a Zeiss Duo Laser Scanning Confocal System (Carl Zeiss, Thornwood, NY, USA), equipped with an C-Apochromat ×40/1.20 W Korr objective. The fluorescence was excited with argon (488 nm) laser output and emitted light measured at wavelengths of > 505 nm with the BP 505–550 filter. The intensity of the illuminating laser intensity was attenuated to 1%.

Isolation of myofibres from FDB muscle

Mice were anaesthetized and FDB muscles were harvested bilaterally. Single myofibres were enzymatically isolated in Dulbeccos' modified Eagle's medium and 2 mg ml^{-1} type II collagenase (Gibco, Thermo Fisher Scientific, Waltham, MA, USA) for 2 h at 37°C. Tissue was tranferred to FDB medium (Dulbecco's modified Eagle's medium with 2% BSA, 1μl ml^{-1} gentamicin, and 1μl ml^{-1} fungizome), triturated, and incubated for 12–24 h. Myofibres were plated on 96-well plates coated with laminin (Sigma-Aldrich, St Louis, MO, USA) 1 h before experimentation. When muscles had been electroporated, a period of 2 weeks was allowed for recovery prior to dissection of the FDB muscles.

Before the experiment, the fibres were washed in normal Tyrode solution, pH 7.4, containing 140 mM NaCl, 5 mM KCl, 0.5 mM $MgCl_2$, 0.3 mM NaH_2PO_4, 5 mM Hepes, 5.5 mM glucose, 1.8 mM $CaCl_2$. Tyrode solution free of Ca^{2+} was prepared without $CaCl_2$.

Confocal imaging

Isolated FDB fibres were loaded with Rhod-2AM (Thermo Fisher Scientific) for 45 min in the culture medium at 37°C and then washed with Tyrode solution. Trains of voltage-induced Ca^{2+} transients were induced by field stimulation (1 Hz for 10 s) every 1 min for 5 min with a custom-designed electrode/microperfusion apparatus (gift of C. Ward, School of Nursing, University of Maryland, Baltimore). Control experiments, done in the presence of 50 μM *N*-benzyl-*p*-toluene sulfonamide to inhibit contraction, gave identical results.

Rhod-2 was visualized with the Zeiss Duo confocal microscope, as described above. The fluorescence was excited with a 560 nm laser and emitted light measured at wavelengths of > 575 nm with the LP 575 filter. The intensity of the illuminating laser was attenuated to 0.5%. All perfusions and imaging were performed in the dark. More than 90% of the myofibres of either genotype responded to voltage pulses by generating Ca^{2+} transients.

Line scan images were acquired in the middle of myofibres at a rate of 1.9 ms per line with the aperture of the confocal detector set to maximum. We used ImageJ 1.31v (NIH, Bethesda, MD, USA) to average the profiles for every pixel in time and took the maximal value for each of 10 voltage pulses to determine the mean maximal value of the Ca^{2+} transients, which were 225 pixels wide under the conditions we used. The values reported were measured as the difference between maximal fluorescence intensity (F_{max}) and background fluorescence (F_o), normalized to F_o.

We found that the amplitudes of the Ca^{2+} transients in electroporated myofibres are higher than those in controls. The reasons for this are unclear and have not been elucidated by DiFranco *et al.* (2011), who studied the effects of electroporation on FDB myofibres. We therefore analysed results from the two types of experiments separately, with different statistical methods: Student's paired *t* test for transfected cells, to compare regions that expressed the transgene with regions that did not, and a simple *t* test for cells that were not transfected.

For *x*–*y* imaging, images (512 × 512 pixels, 0.18 ms per line) were recorded for 5 s at a rate of 10 Hz.

Osmotic shock injury

Cultured FDB fibres were bathed in normal Tyrode solution and then perfused for 45 s with a hypotonic Tyrode solution (see above) containing 70 mM NaCl and maintained in that solution for an additional 15 s. Cells were then bathed in isotonic Tyrode solution for

5 min. Optimal times for injury and recovery from OSI were found in preliminary studies to be 1 and 5 min, respectively, and these conditions were used in all studies requiring OSI. Experiments were performed at room temperature (21–23°C). Data were collected from muscle fibres from at least three mice.

Statistical analysis

Quantitative data are shown as means ± SEM. Student's *t* test was used to compare the data before and after drug interventions. A value of $P < 0.05$ was considered statistically significant.

Materials

S107 was the generous gift of ARMGO Pharma, Inc. (Tarrytown, NY, USA). Unless specified otherwise, all other chemicals were from Sigma-Aldrich. Antibodies to junctophilins 1 and 2 were from Invitrogen (Carlsbad, CA, USA) and Abcam (Cambridge, UK), respectively.

Results

Voltage-induced Ca^{2+} transients in dysferlin-null and control myofibres

We first examined the amplitudes of the voltage-induced Ca^{2+} transients in cultured FDB myofibres from dysferlin-null A/J mice and from A/WySnJ (A/W) controls (Fig. 1*A–D*). The mean amplitude of the transients in A/J fibres was ∼20% less than in A/W fibres (2.0 ± 0.08 *vs.* 2.6 ± 0.08 relative units, $n = 137$ for each group of data, $P < 0.001$). These differences, obtained with the Ca^{2+}-sensitive dye, Rhod-2, are consistent with our earlier results, obtained with Fluo-4 (Kerr *et al.* 2013).

We used electroporation to introduce plasmid DNA encoding V-Dysf into A/J myofibres to learn if the decrease in the amplitude of the voltage-induced Ca^{2+} transients could be corrected by the expression of dysferlin. As controls, we used A/J and A/W myofibres electroporated to express Venus alone ($n = 14$ and $n = 10$, respectively). Although Venus alone is expressed throughout the fibre (Fig. 1*E*), the expression of the V-Dysf transgene was highly localized after electroporation (Fig. 1*F*). Where it was expressed, it concentrated in doublets at the level of the A–I junction (Fig. 1*F* inset), consistent with our previous results and with its presence in the T-tubules of skeletal muscle (Roche *et al.* 2011; Kerr *et al.* 2013). We therefore limited our analysis to regions that showed either high Venus fluorescence or no detectable fluorescence.

Our results indicate the voltage-induced Ca^{2+} transients in the regions of A/J fibres that express V-Dysf were ∼20% greater (paired *t* test, $n = 38$, $P < 0.01$) in amplitude than transients in non-transfected regions of the fibres. Comparison of the voltage-induced Ca^{2+} transients in A/J fibres transfected with V-Dysf ($n = 38$) and in A/J fibres transfected with Venus ($n = 27$) showed a difference of 38% (Fig. 1*G* and *H*; 5.1 ± 0.27 *vs.* 3.2 ± 0.43 relative units, $P < 0.01$). Although the amplitudes of the Ca^{2+} transients in electroporated fibres were higher than in those that were not electroporated, the relative changes in amplitudes in the two preparations were similarly dependent on dysferlin. Thus, the effect is specific for dysferlin.

Effects of Ca^{2+}-channel inhibitors on voltage-induced Ca^{2+} transients

We next examined the effects of several different classes of inhibitors of the LTCC (diltiazem, a benzothiazapine; nifedipine, a dihydropyridine; verapamil, a phenylalkylamine) and of the RyR1 (tetracaine, an anaesthetic; dantrolene, a derivative of aminohydantoin) on the voltage-induced Ca^{2+} transients of A/J and A/W myofibres in culture. Studies of the concentration dependence of inhibition on the amplitudes of the voltage-induced Ca^{2+} transients by each of these drugs gave a range of values for half-maximal inhibition, from 3 μM for tetracaine to 67 μM for diltiazem (Fig. 2). With the exception of diltiazem (see below), each drug interacted with A/J and A/W fibres similarly; the small differences we observed were not statistically significant.

As the concentrations of drugs that strongly inhibited voltage-induced Ca^{2+} transients were well above their physiologically effective ranges, which in skeletal muscle are typically in the 1–10 μM range (Walsh *et al.* 1986; Williams, 1990; Kerr *et al.* 2013), we limited our studies to lower concentrations. Of the drugs we assayed, diltiazem at 5–10 μM was unique in its ability to increase the amplitude of the voltage-induced Ca^{2+} transients of A/J but not A/W fibres (Fig. 2*A*; increase of ∼20% at 10 μM), suggesting that it potentiates the release of Ca^{2+} in response to voltage pulses, as reported (Gonzalez-Serratos *et al.* 1982). Notably, this effect was not seen in A/J fibres electroporated to express V-Dysf (Fig. 2*B*). The differences in the amplitudes of the voltage-induced Ca^{2+} transients at 5 and 10 μM diltiazem between A/J and A/W (Fig. 2*A*), A/J and A/J expressing V-Dysf (Fig. 2*B*), and A/J and A/J treated with diltiazem ($n = 29$ and $n = 22$ for 5 and 10 μM, respectively, $P < 0.005$) were statistically significant. This suggests that the increase in amplitude of the voltage-induced Ca^{2+} transients in A/J fibres by dysferlin can be at least partially mimicked by diltiazem.

Osmotic shock injury

We reported previously that injury by brief hypoosmotic shock (OSI) led to a decrease in the amplitude of voltage-induced Ca^{2+} transients in A/J myofibres *in vitro* that was severalfold greater than the decrease in A/W

fibres (Kerr *et al.* 2013). We used OSI to determine if the expression of dysferlin in A/J fibres was sufficient to protect against the loss of amplitude of the Ca^{2+} transients. Figure 3 shows representative Ca^{2+} transients in A/W (Fig. 3*A* and *B*) and A/J (Fig. 3*C* and *D*) fibres, and in A/J fibres transfected with V-Dysf (Fig. 3*E*), before and 5 min after OSI. The recovery of voltage-induced Ca^{2+} transients in A/J fibres was significantly lower than recovery in A/W fibres, as reported (Kerr *et al.* 2013). Expression of V-Dysf in A/J fibres rendered the A/J fibres resistant to loss of transient amplitude as A/W (Fig. 3*E*), but only in the regions of the myofibres in which V-Dysf was expressed (Fig. 3*F*). Transfection of A/J myofibres with Venus alone failed to yield any protection (Fig. 3*F*). This indicates that dysferlin specifically protects A/J myofibres from the loss of amplitude of the voltage-induced Ca^{2+} transients that typically occurs during and after OSI.

Effects of inhibitors during OSI

We showed previously that treatment of A/J fibres with 10 μM diltiazem was sufficient to prevent the loss of

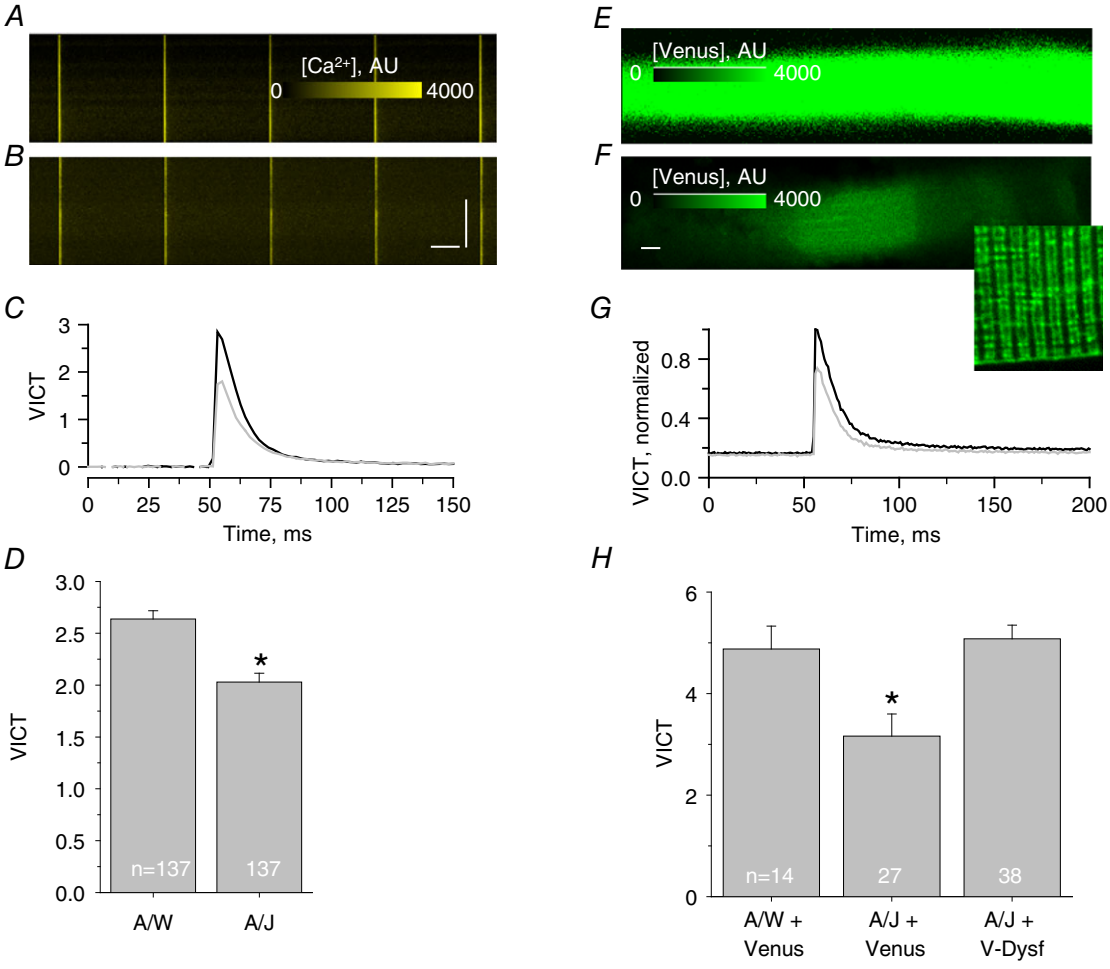

Figure 1. Amplitude of the voltage-induced Ca^{2+} transients in A/J and in A/W fibres with and without transfection

A and *B*, representative line-scan confocal images of voltage-induced Ca^{2+} transients (Rhod-2 fluorescence) in A/W (*A*) and A/J (*B*) FBD fibres. Bars, 100 μm (vertical) and 250 ms (horizontal). *C*, corresponding profiles of voltage-induced Ca^{2+} transients from the images *A* and *B* presented as $(F_{max} - F_o)/F_o$. Black line, A/W; grey line, A/J. *D*, averaged amplitude of voltage-induced Ca^{2+} transients in A/W and A/J fibres, presented as $(F_{max} - F_o)/F_o$. Number of experiments is in white; $^*P < 0.001$ compared to A/W. *E* and *F*, representative *x–y* confocal fluorescence images of A/J FBD fibres after transfection with Venus (*E*) or V-Dysf (*F*). *G*, representative profiles of voltage-induced Ca^{2+} transients from fibre areas transfected with V-Dysf (black line) or non-transfected (grey line). The voltage-induced Ca^{2+} transients are normalized to F_{max} in the area transfected with V-Dysf. *H*, averaged amplitude of voltage-induced Ca^{2+} transients in A/W and A/J fibres presented as $(F_{max} - F_o)/F_o$. Number of experiments is in white; $^*P < 0.05$ compared to V-Dysf; bars, 10 μm. [Colour figure can be viewed at wileyonlinelibrary.com]

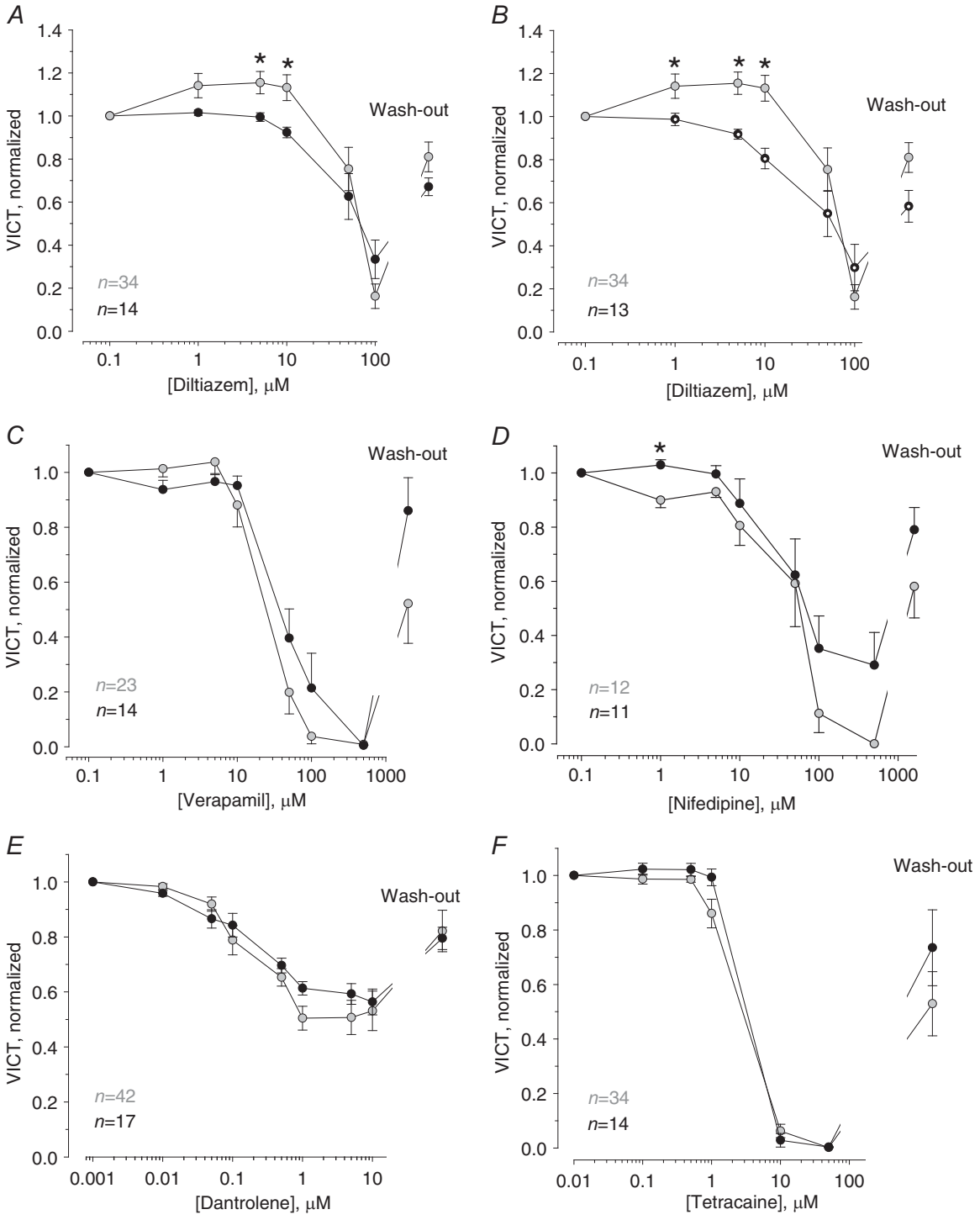

Figure 2. Effects of Ca^{2+} channel inhibitors on voltage-induced Ca^{2+} transients in A/W and A/J fibres
A, effects of diltiazem on voltage-induced Ca^{2+} transients in A/W (black circles) and A/J (grey circles) FDB fibres. *B*, effects of diltiazem on voltage-induced Ca^{2+} transients in A/J (grey circles) fibres and A/J muscle fibres transfected with wild-type dysferlin (black open circles). *C–F*, dose-dependent effects of verapamil (*C*), nifedipine (*D*), dantrolene (*E*) and tetracaine (*F*) on voltage-induced Ca^{2+} transients in A/W (black circles) and A/J (grey circles) fibres. Number of experiments are given for corresponding colour; $^*P < 0.05$ to corresponding value at the same concentration.

amplitude of the voltage-induced Ca^{2+} transients caused by OSI (Kerr *et al.* 2013). As LTCCs are blocked by diltiazem, this suggested that LTCCs are involved in the response of dysferlinopathic fibres to injury. Diltiazem can act on channels other than LTCCs, however (Caballero *et al.* 2004). To explore the mechanisms underlying dysferlinopathy further, we examined the effects of low concentrations of diltiazem and other Ca^{2+} channel blockers, which act either on the LTCC or the RyR1 of skeletal muscle, on the response of A/J fibres to OSI.

Figure 4 shows the effects of low concentrations of diltiazem, verapamil, nifedipine, dantrolene and tetracaine on the loss of voltage-induced Ca^{2+} transients in A/J FDB fibres exposed to OSI. All the drugs completely or nearly completely blocked the loss of the transients at concentrations of 10 μM or less. Notably, nifedipine at 5 μM and verapamil at 10 μM were approximately as effective as diltiazem at 10 μM. In addition, 10 μM dantrolene (Fig. 4*B*) and 1 μM tetracaine (Fig. 4*B*) fully protected the transients after OSI. A higher concentration of tetracaine (10 μM) was also protective, but because it is itself inhibitory, it had to be washed out before recovery of the voltage-induced Ca^{2+} transients could be measured. Figure 4*C* shows that washout of 10 μM tetracaine was essentially accomplished by 10 min following OSI, and that recovery of the transient amplitude was complete and indistinguishable from uninjured A/J or injured A/W fibres.

Our observation that inhibitors of the LTCC (diltiazem, nifedipine, verapamil) and of the RyR1 (dantrolene, tetracaine) protect A/J fibres from OSI-induced loss of voltage-induced Ca^{2+} transients strongly suggests that the damage caused to the voltage-induced Ca^{2+} transients requires both proteins.

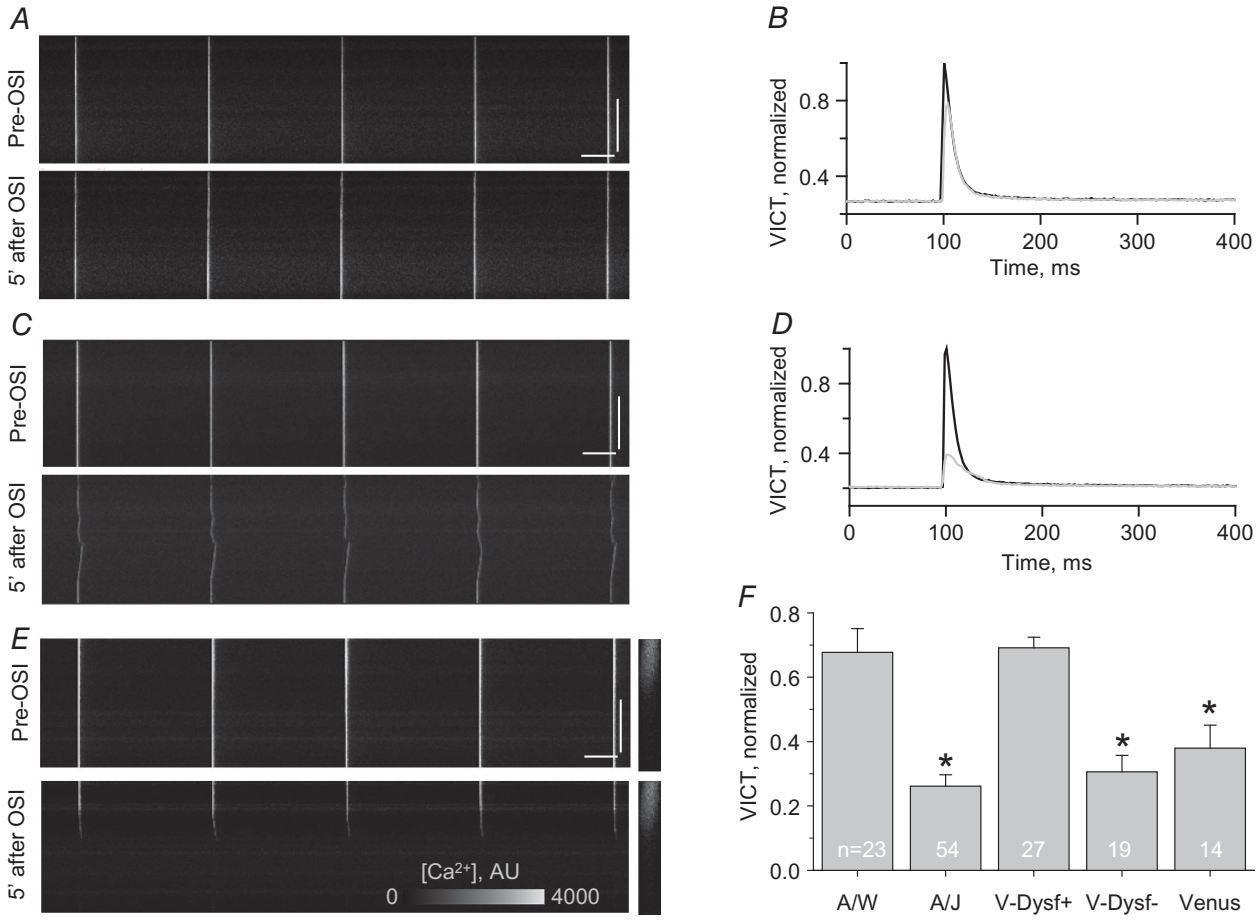

Figure 3. Effect of osmotic shock on Ca^{2+} transients in FBD fibres
A, *C* and *E*, representative line-scan confocal images of voltage-induced Ca^{2+} transients in A/W (*A*) and A/J (*C*) FBD fibres and A/J fibres transfected with V-Dysf (*E*) before and 5 min after OSI. Distribution of V-Dysf, introduced by electroporation and seen as Venus fluorescence, is shown on *x–y* images located on the right of panel *E*. *B* and *D*, corresponding profiles of voltage-induced Ca^{2+} transients from the images presented in *A* and *C* for pre-OSI (black line) and 5 min after OSI (grey line). Transients are normalized to F_{max} for pre-OSI conditions. *F*, averaged data for recovery of Ca^{2+} transients in FBD fibres under the different conditions used. Number of experiments in white; $^*P < 0.005$ compared to A/W; bars, 100 μm (vertical) and 250 ms (horizontal).

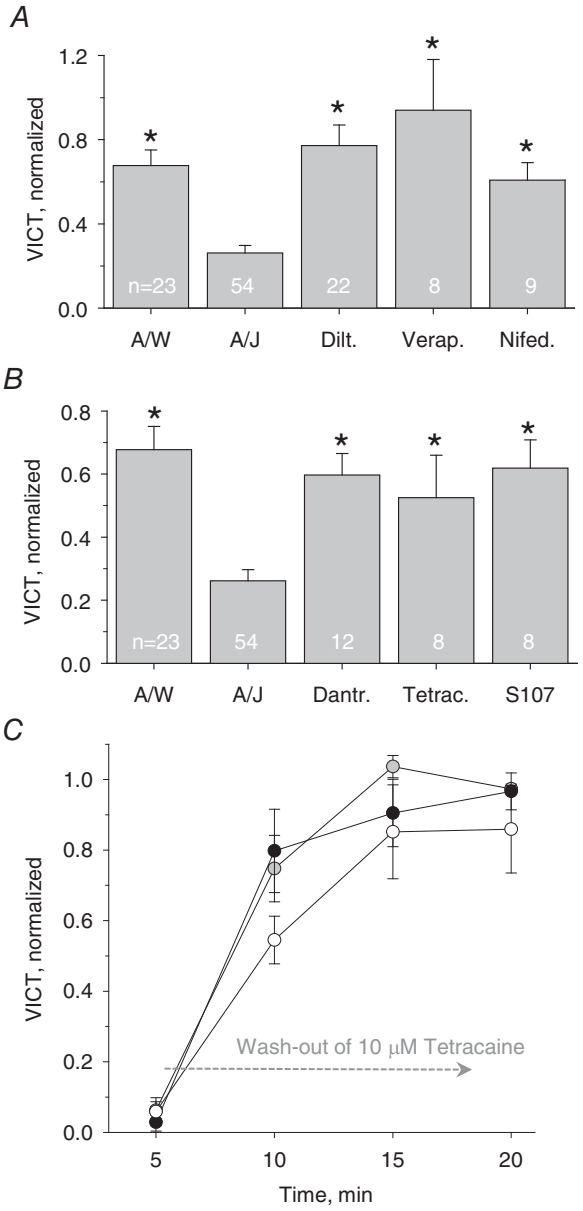

Figure 4. Effects of pharmacological agents on recovery of voltage-induced Ca^{2+} transients in A/J fibres after OSI
A, averaged data for recovery of Ca^{2+} transients in FBD fibres in the presence of 10 μM diltiazem (Dilt.), 10 μM verapamil (Verap.) or 5 μM nifedipine (Nifed). *B*, averaged data for recovery of Ca^{2+} transients after OSI in FBD fibres in the presence of 10 μM dantrolene (Dantr.), 1 μM tetracaine (Tetrac.) or 10 μM S107. Number of experiments is shown in white; $^*P < 0.05$, compared to A/J. The two bars to the left duplicate those in *A*. *C*, averaged data for recovery of voltage-induced Ca^{2+} transients during wash-out of 10 μM tetracaine for A/W (no OSI; black circles) and A/J (no OSI; grey circles) fibres, and for A/J fibres after OSI (open circles). Data points are means of 6–27 independent experiments.

Effects of prevention of Ca^{2+} leak through RyR1 with S107

As flow of Ca^{2+} from the lumen of the SR through the RyR1 appears to be required for the OSI-induced loss of amplitude of voltage-induced Ca^{2+} transients in dysferlin-null muscle fibres, we tested the effects of S107, which inhibits spontaneous Ca^{2+} leak through the RyR by stabilizing the binding of FK506 binding protein (FKBP; Andersson *et al.* 2012). S107 had no effect on the amplitude of voltage-induced Ca^{2+} transients in A/J fibres that were not subjected to OSI, or to A/W fibres before or after OSI ($n = 12$; not shown). With A/J fibres subjected to OSI, however, S107 added before and during injury largely protected against the OSI-induced decrease in amplitude of voltage-induced Ca^{2+} transients (Fig. 4*B*). These results support a role for Ca^{2+} leak through the RyR1 in the pathophysiology of injured dysferlin-null muscle, consistent with our results with dantrolene and tetracaine.

Ca^{2+}-free medium

We investigated the possible contribution of extracellular Ca^{2+} to the loss of amplitude of voltage-induced Ca^{2+} transients of A/J myofibres, and the effects on A/J fibres of OSI, by removing all the Ca^{2+} from the Tyrode solution bathing the myofibres. The amplitude of the voltage-induced Ca^{2+} transients in A/W and A/J myofibres was not affected by Tyrode solution lacking Ca^{2+}, compared to normal Tyrode solution (1.8 mM Ca^{2+}, $n = 7$ for each). Similarly, OSI had the same inhibitory effect on the voltage-induced Ca^{2+} transients of A/J myofibres whether Ca^{2+} was present or absent in the medium (Fig. 5). The recovery of the transients after OSI in Ca^{2+}-free Tyrode solution was $28 \pm 10\%$ ($n = 5$), similar to recovery in normal Tyrode solution. These results suggest that the influx of Ca^{2+} from the medium into the myoplasm does not play a major role in the voltage-induced Ca^{2+} transients or in the decrease in the transients in dysferlin-null muscle following OSI.

Ca^{2+} waves and Ca^{2+} sparks in A/J fibres after OSI

The minimal role for extracellular Ca^{2+}, and the protective effects of S107 and the other drugs that target the LTCC and RyR1 directly, suggest that intracellular Ca^{2+} homeostasis is dysregulated in injured A/J fibres. As dysregulation can be accompanied by Ca^{2+} waves and Ca^{2+} sparks, especially in cardiac myocytes (e.g. Lukyanenko & Gyorke, 1999) but also in skeletal myofibres (Bellinger *et al.* 2009; Andersson *et al.* 2012), we searched for these in injured A/J fibres. We found that 44.4% of A/J fibres ($n = 27$) at 5 min after OSI demonstrated spreading waves of Ca^{2+}. Figure 6 shows representative confocal images of the voltage-induced Ca^{2+} transients and Ca^{2+} waves in

A/J fibres before and at different time intervals after OSI. Enlarged images of single Ca^{2+} transients (Fig. 6, right panels) show that even at 20 min after OSI the transients continued to be 'wavy' in appearance. Figure 7*A* and Supplementary Video 1 show waves moving through a region of an injured A/J fibre first in one direction and then in the opposite direction, consistent with a coordinated release of Ca^{2+} over a significant volume of the fibre.

Figure 7*B* shows evidence for spontaneous Ca^{2+} sparks and Ca^{2+} bursts in injured A/J myofibres. Sparks occurred at the time of voltage stimulation (yellow arrows) or spontaneously (white arrows), suggesting a similar underlying mechanism. Some positions across the myofibres showed repetitive Ca^{2+} sparks. Bursts (green arrows) are less frequent. Scans of individual spark and burst events are shown in Fig. 7*C*. Although we have not yet fully characterized these events, they are very similar to those reported in both skeletal and cardiac muscle cells. These events, as well as the Ca^{2+} waves illustrated above, indicate that control of Ca^{2+} release is significantly altered in injured dysferlin-null myofibres.

Figure 8 shows that expression of V-Dysf fully protected A/J fibres against the OSI-induced Ca^{2+} waves ($n = 6$) in the regions where V-Dysf was expressed. Furthermore, treatment of A/J fibres with 10 μM S107 before and during OSI reduced the number of fibres with Ca^{2+} waves 4-fold (to 11.1%, $n = 9$).

Differences in Ca^{2+} signalling in A/J muscle are not linked to proteolysis

Elevated levels of cytoplasmic Ca^{2+} in skeletal muscle can activate calpain 3, leading to degradation of junctophilins (e.g. Murphy *et al.* 2013). We tested the possible role of calpains in the loss of the Ca^{2+} transient in A/J muscle following OSI by preincubating the fibres in 50 μM calpeptin, a calpain inhibitor. We found no protection against the loss in amplitude (Fig. 9*A* and *B*). Immunoblots further showed that both junctophilin 1 and junctophilin 2 are present at similar levels in A/J and control muscles (Fig. 9*C*), suggesting that differences in their degradation do not account for the differences in the amplitudes of the Ca^{2+} transients before injury.

Discussion

The role of dysferlin in skeletal muscle and the mechanisms underlying muscular dystrophies associated with mutations in the *DYSF* gene have been controversial. Our previous results showed that most of the dysferlin present in mature skeletal muscle fibres concentrates in the T-tubules, where it stabilizes Ca^{2+} release at the triad junction when muscle is injured either *in vitro* or *in vivo*. We also found that diltiazem, which blocks the L-type Ca^{2+} channel (LTCC) in muscle without inhibiting excitation–contraction coupling (Gonzalez-Serratos *et al.* 1982; Williams, 1990; Böhle, 1992), protects dysferlin-null murine muscle against injury *in vitro* and *in vivo* (Kerr *et al.* 2013). These results suggest that Ca^{2+} signalling is defective in injured dysferlin-null muscle, but the mechanisms by which Ca^{2+} accesses the myoplasm under pathogenic conditions, how these conditions can lead to long-term, possibly self-perpetuating, effects, and how dysferlin suppresses pathology remain unknown. Here we report studies on Ca^{2+} release by injured dysferlin-null muscle fibres *in vitro* that begin to address these questions. We found that dysferlin itself improves Ca^{2+} release when it is expressed in the dysferlin-null background, and that this increase is mimicked by low concentrations of diltiazem. Our results further indicate that, upon injury of dysferlin-null myofibres in culture, most of the Ca^{2+} that accesses the myoplasm from the lumen of the SR is associated with Ca^{2+} leak from the SR that is suppressed by the expression of dysferlin. We suggest that the absence of dysferlin leads to changes in coupling between the LTCC

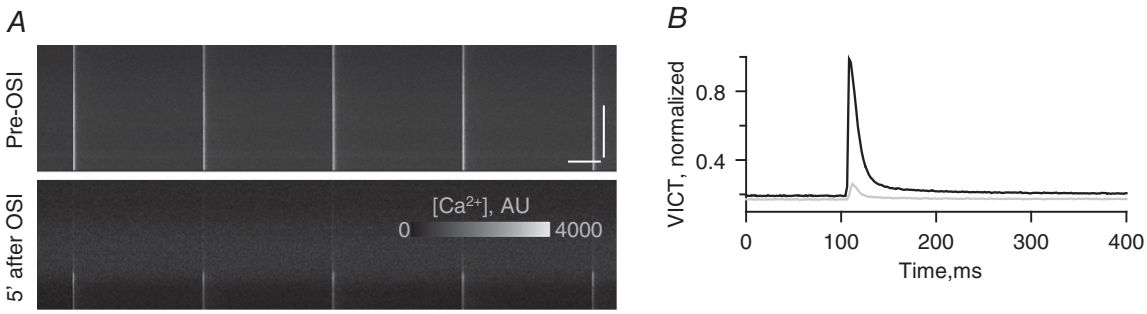

Figure 5. Effect of Ca^{2+}-free Tyrode solution on recovery of voltage-induced Ca^{2+} transients from OSI in A/J fibres
A, representative line-scan confocal images of the voltage-induced Ca^{2+} transients in A/J FBD fibres before and after OSI in nominally Ca^{2+}-free Tyrode solution. *B*, corresponding profiles of transients from the images presented on *A* for pre-OSI (black) and 5 min after OSI (grey) conditions. Voltage-induced Ca^{2+} transients are normalized to F_{max} for pre-OSI conditions. Bars, 100 μm (vertical) and 250 ms (horizontal).

and the RyR1, which can in turn contribute significantly to the pathology of dysferlinopathies.

Role of extracellular and SR Ca^{2+}

Our pharmacological studies with three specific inhibitors of the LTCC, diltiazem, nifedipine and verapamil, indicate that the LTCC plays an important role in the response of dysferlin-null muscle to OSI (Fig. 4*A*). The three drugs are chemically distinct, but they all bind at nearby sites on the $\alpha 1$ subunit of the LTCC (Döring *et al.* 1996; Hering *et al.* 1996; Peterson *et al.* 1997; Hockerman *et al.* 1997, 2000). Their binding blocks the flux of Ca^{2+} through the channel and thereby reduces the concentration of Ca^{2+} in the narrow cleft of the triad junction. In our experiments (Fig. 2), low concentrations of these drugs ($\leq 10\ \mu$M) do not reduce the size of the voltage-induced Ca^{2+} transient, however, consistent with the idea that they do not interfere significantly with the biomechanical coupling of the LTCC and the RyR1 that is essential for the normal release of Ca^{2+} required to initiate contraction (e.g. Lamb, 1986; reviewed in Rios *et al.* 2015; Bannister, 2016). Thus, their effects on control muscle are benign under normal circumstances but are highly beneficial in protecting dysferlin-null muscle from injury. Further studies will be needed to determine if other drugs of the dihydropyridine, phenyalkylamine or benzothiazepine families, or indeed drugs of other chemical families that target the LTCC, share these effects.

Of these drugs, diltiazem has the most distinctive effect on dysferlin-null muscle, as it actually increases the amplitude of the voltage-induced Ca^{2+} transients in uninjured, dysferlin-null muscle. The magnitude of the increase, ~20%, is sufficient to restore the amplitude to that of wild-type A/W muscle. Restoration of expression of dysferlin similarly restores the magnitude of the voltage-induced Ca^{2+} transients to control levels while also eliminating the stimulatory effect of diltiazem. These results suggest that the absence of dysferlin, rather than other minor genetic differences between A/J and

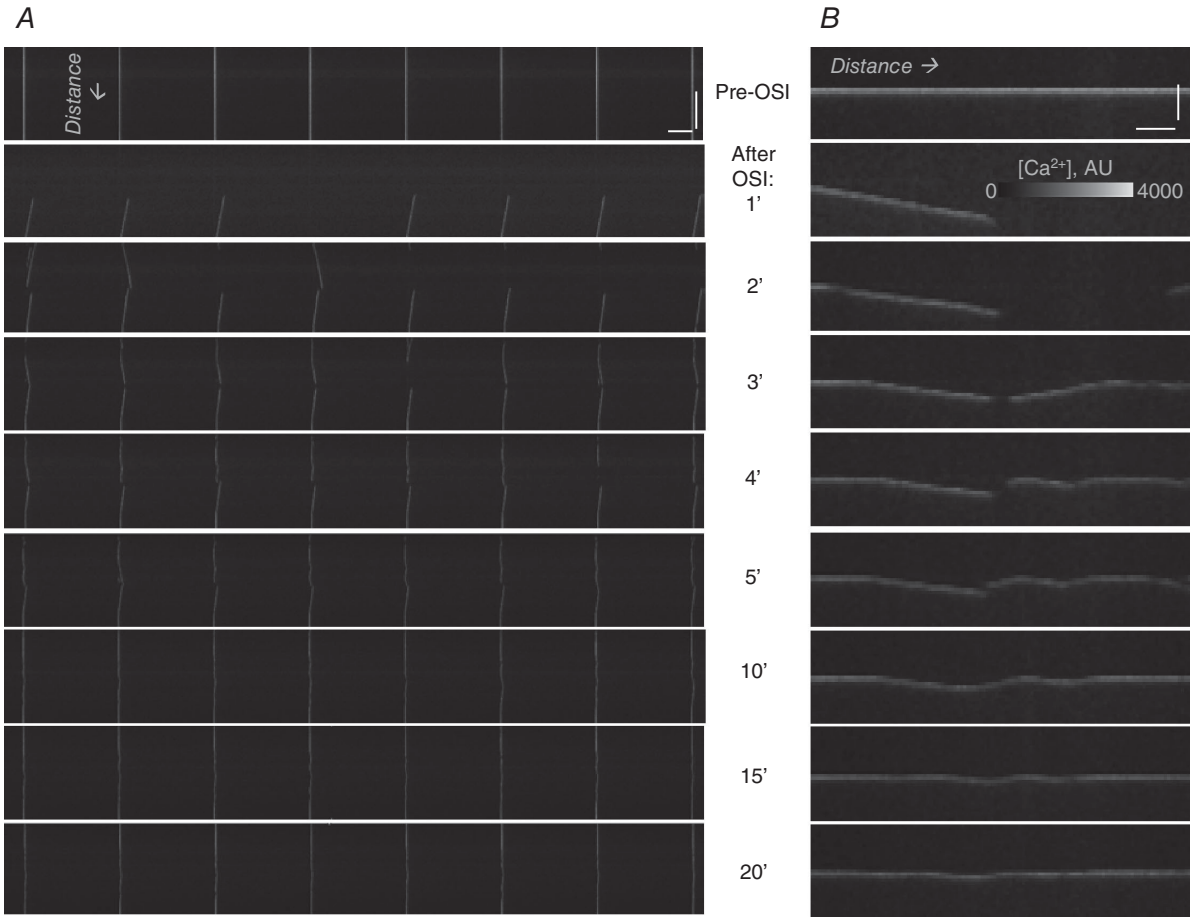

Figure 6. Ca^{2+} waves in A/J fibres after OSI
A, representative line-scan confocal images of the voltage-induced Ca^{2+} transients and Ca^{2+} waves in A/J fibres before and after OSI. Time (in minutes) after OSI is shown between panels. *B*, enlarged images of Ca^{2+} signals, reoriented with the initial time of stimulation at the upper left of each panel. Bars: left panel, 100 μm (vertical) and 250 ms (horizontal); right panel, 100 ms (vertical) and 25 μm (horizontal).

A/W mice, is sufficient to reduce the amplitude of the voltage-induced Ca^{2+} transient, and that diltiazem can mimic the effect of dysferlin in increasing the transient as well as protecting against damage caused by OSI. The effect of diltiazem also suggests that the LTCC and RyR1 in dysferlin-null muscle can be coupled biomechanically at full efficiency without changes in gene expression, as required in ageing muscle (Wang *et al.* 2002).

Consistent with our results, diltiazem at micromolar concentrations has previously been reported to enhance the binding of DHPR antagonists, PN 200-110 and nimodipine, to skeletal muscle membranes in

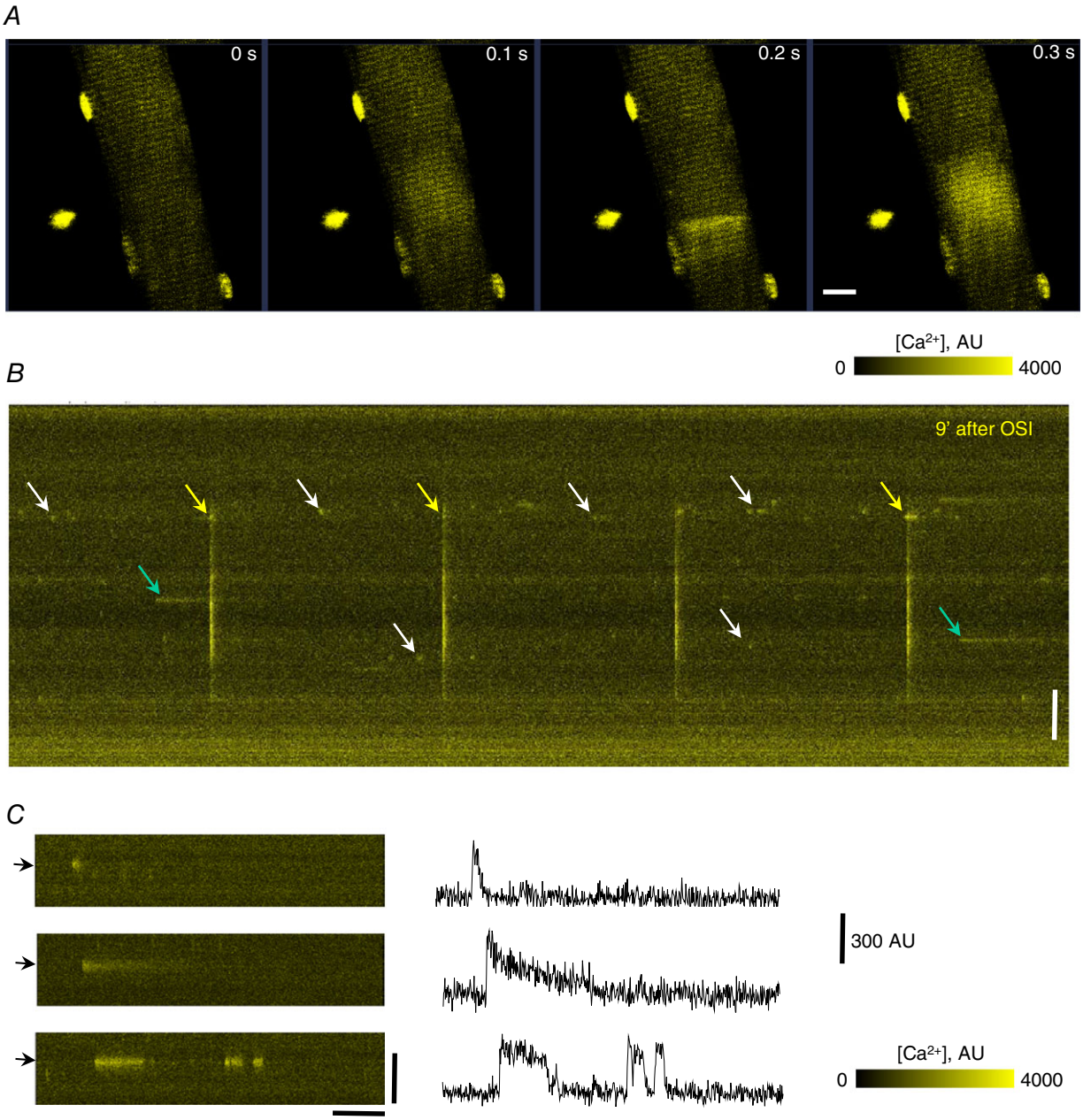

Figure 7. Spontaneous Ca^{2+} waves and sparks in A/J fibres after OSI
A, representative *x–y* scans of confocal images of spontaneous Ca^{2+} wave in A/J fibres after OSI as a function of time (in seconds). Bar, 10 μm. *B*, line-scan confocal images of the voltage-induced Ca^{2+} transients, and voltage-induced (yellow arrows) and spontaneous (white arrows) Ca^{2+} sparks and bursts (green arrows) visualized at 9 min after OSI. The arrowhead indicates a location at which sparks arise repeatedly. Bars, 20 μm (vertical) and 250 ms (horizontal). *C*, representative Ca^{2+} sparks and bursts shown at higher magnification at 15 min after OSI. On the right are plotted time-dependent changes in $[Ca^{2+}]$, recorded by averaging a 2 μm line at sites indicated by arrows. Bars, 10 μm (vertical) and 300 ms (horizontal). [Colour figure can be viewed at wileyonlinelibrary.com]

a stereospecific manner (Goll *et al.* 1983; Ferry & Glossmann, 2016). It also increases the amplitude of the voltage-induced Ca^{2+} transient in frog muscles (Gonzalez-Serratos *et al.* 1982). Notably, frog muscles have not been shown to contain dysferlin. In addition, the T-tubule system in amphibian muscles is present at the level of the Z-disk, near the sarcoplasmic reticulum, rather than displaced to the A–I junction, as it is in mammalian skeletal muscle. A similar situation pertains in mammalian heart muscle, which is spared in most cases of dysferlinopathy (Takahashi *et al.* 2013; Nishikawa *et al.* 2016). Both factors may contribute to diltiazem's enhancement of the amplitude of the voltage-induced Ca^{2+} transients in wild-type frog muscle but only in dysferlin-null mouse muscle.

Although our results strongly implicate a role for the LTCC in the response of dysferlin-null muscle fibres to OSI, they suggest that Ca^{2+} flux through the channel is only a minor contributor to injury. In particular, removal of extracellular Ca^{2+} does not protect A/J myofibres from loss of the Ca^{2+} transient following OSI (Fig. 5). Thus, Ca^{2+} entry is unlikely to play a significant role in the changes in the Ca^{2+} transient induced by OSI in the absence of dysferlin. These results also suggest that other pathways for influx of extracellular Ca^{2+}, such as stretch-activated or Trp channels, are unlikely to be involved. This is consistent with the much higher concentrations of tetracaine needed to block Trp channels (Zholos, 2010). Higher concentrations of tetracaine have been used to block voltage-gated Na^{+} channels as well (Tamkun *et al.* 1984; Brown *et al.* 2009; but see Aksentsev *et al.* 1983; Braü *et al.* 1998).

The effect of nominally Ca^{2+}-free medium on the loss of the Ca^{2+} transient after OSI differs from our previous observation (Kerr *et al.* 2013) that extracellular Ca^{2+} is required for the prolonged retention of the impermeant dye sulforhodamine B in the T-tubules of A/J myofibres after OSI. We speculate that this difference is due to differences in the requirement for Ca^{2+} in promoting membrane sealing (e.g. Bansal *et al.* 2003; McNeil *et al.* 2003), as distinct from maintaining mechanochemical coupling between the LTCC and the RyR1 following injury.

As shown by Pickering *et al.* (2009), the aftermath of OSI of healthy rat myofibres includes increases in cytoplasmic Ca^{2+} that induce Ca^{2+} sparks. They also show that this effect is blocked by nifedipine and tetracaine, consistent with our current results. We propose that in the absence of dysferlin, OSI induces a larger change in cytoplasmic Ca^{2+} than in healthy muscle, leading to more extensive disruption of the mechanochemical coupling of the LTCC to the RyR1, and accompanying decreases in the amplitude of the Ca^{2+} transient. The enhanced leak of Ca^{2+} from the SR lumen through the RyR1 into the cytoplasm that occurs upon OSI might then be sufficient to lead to the generation of Ca^{2+} sparks and waves. The predominant role of the

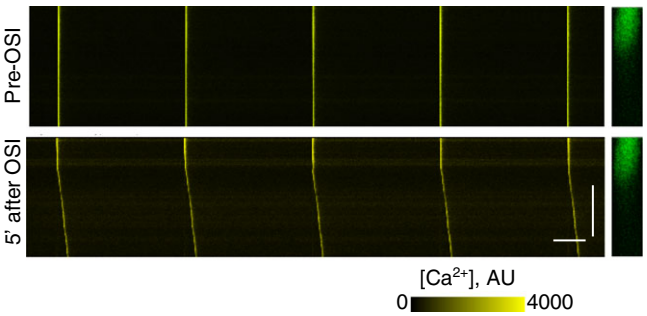

Figure 8. V-Dysf suppresses the development of Ca^{2+} waves in A/J fibres after OSI
Representative line-scan confocal images of the voltage-induced Ca^{2+} transients and Ca^{2+} waves in A/J fibres showing regional expression of V-Dysf before and 5 min after OSI. Distribution of V-Dysf, seen as Venus fluorescence, is shown on *x–y* images to the right. Bars, 100 μm (vertical) and 250 ms (horizontal). [Colour figure can be viewed at wileyonlinelibrary.com]

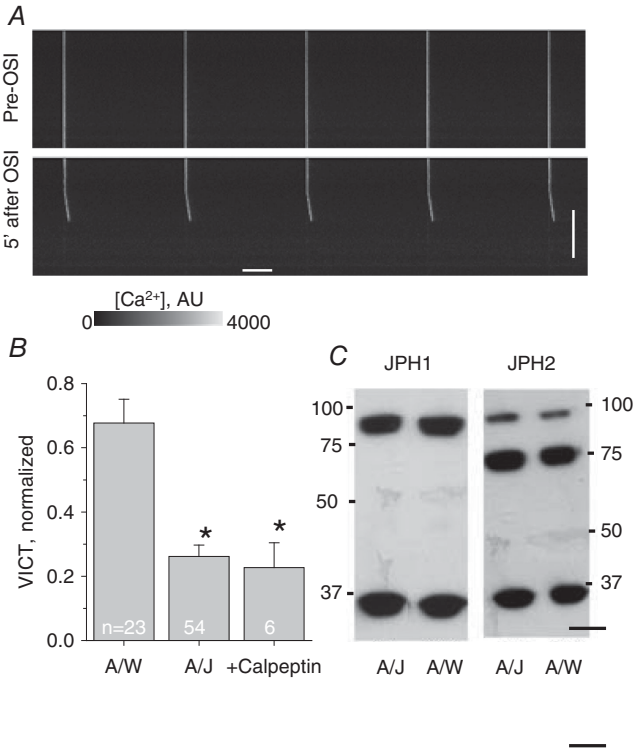

Figure 9. Evidence against proteolysis in A/J fibres
A, representative line-scan confocal images of the voltage-induced Ca^{2+} transients and Ca^{2+} waves before and 5 min after OSI in A/J fibres pretreated for 1 h with 50 μM calpeptin. *B*, averaged data for recovery of Ca^{2+} transients in A/J FBD fibres pretreated and not pretreated with 50 μM calpeptin in comparison to A/W FBD fibres. Number of experiments is shown in white; $*P < 0.005$ compared to A/W. Bars, 100 μm (vertical) and 250 ms (horizontal). *C*, representative SDS-PAGE shows amount of junctophilins 1 or 2 (JPH1 or JPH2) in A/J and A/W muscle fibres. Molecular mass markers, in kDa, are indicated. Glyceraldehyde phosphate dehydrogenase is the loading control, at 36 kDa.

RyR1 and the leak of Ca^{2+} that it mediates can account for our results with dantrolene and tetracaine, which we used at concentrations that do not significantly inhibit the voltage-induced Ca^{2+} transient in healthy myofibres (Fig. 2). Both inhibit Ca^{2+} flux through the RyR1 (Fruen *et al.* 1997; Brum *et al.* 2003) and both protect A/J fibres from the effects of OSI (Fig. 4*B*).

We used S107 to test this possibility further. S107 stabilizes the binding of FKBP (also known as calstabin 1) to the RyR1, which reduces Ca^{2+} leak through the RyR1 without inhibiting its normal biomechanical coupling to the LTCC. It has been used by the Marks laboratory to show that increased Ca^{2+} leak is a significant contributor to other forms of muscular dystrophy, including dystrophinopathy and β-sarcoglycanopathy (Bellinger *et al.* 2009; Andersson *et al.* 2012; see also Takagi *et al.* 1992), as well as to the changes that occur in muscle upon ageing (Andersson *et al.* 2011). Our finding that S107 protects A/J muscle against the effects of OSI (Fig. 4*B*) suggests that increased Ca^{2+} leak through the RyR1 contributes significantly to the injury-induced loss of amplitude of the voltage-induced Ca^{2+} transient.

Increased RyR1 Ca^{2+} leak cannot readily account for all our results, however, as indicated by the effects of diltiazem and other blockers of the LTCC, discussed above. We speculate that the interaction of the LTCC with the RyR1 in dysferlin-null muscle is stabilized by drugs, such as diltiazem, that bind to the channel wall, and that this reduces the susceptibility of RyR1 to leak following osmotic shock injury when dysferlin is absent.

Evidence consistent with abnormal Ca^{2+} release and its possible role in pathogenesis

Higher than normal cytoplasmic Ca^{2+} concentrations in the vicinity of the triad junction can have many potential effects that alter the activity of the RyR, including, in cardiac muscle, Ca^{2+}-induced Ca^{2+}-release (CICR). Ca^{2+} sparks and voltage-induced and spontaneous Ca^{2+} waves are typical of cardiomyocytes in which CICR is dysregulated. Although it does not typically contribute significantly to the transient in healthy skeletal muscle (Shirokova *et al.* 1998; Rios *et al.* 2015), CICR may play a role in caffeine-induced contractures and in some myopathies (Endo, 2009). This possibility is consistent with our observations of Ca^{2+} sparks and waves and, in rare instances, spontaneous Ca^{2+} waves, in injured dysferlin-null myofibres (Figs 6–8). Nevertheless, CICR is not the only mechanism that can account for our data: store overload-induced Ca^{2+} release (SOICR: Jiang *et al.* 2008; Cully & Launikonis, 2016; Wakizaka *et al.* 2017, but see Kong *et al.* 2007) may also do so. SOICR occurs in skinned muscle fibres exposed to high concentrations of Mg^{2+} and leads to Ca^{2+} waves that can last several seconds. Although our observation that osmotic shock injury in nominally Ca^{2+}-free solution does not protect against the loss of the Ca^{2+} transient is inconsistent with store overload, Ca^{2+} sparks and waves can be caused by SOICR and thus are not diagnostic of any particular mechanism underlying increased Ca^{2+} release. We are now planning additional experiments to determine the mechanism(s) that contribute to the increase in Ca^{2+} release in injured dysferlin-null muscle.

The effect of expression of dysferlin in some regions of the fibres, but not others, indicates that the differences between A/J and A/W myofibres under normal conditions (Fig. 1) and after OSI (Figs. 3 and 8) are due primarily to the absence or presence of dysferlin, respectively. Furthermore, they suggest that the control of Ca^{2+} leak and its consequences in injured dysferlin-null muscle fibres is highly localized. After electroporation, V-Dysf tends to concentrate at one end of the transfected FDB muscle fibre. Expression of the V-Dysf fusion protein is apparent up to about 50 μm from the end of the fibre, with little or no detectable fluorescence in the middle of the fibre or at the other end. This creates a heterogeneous environment in which one part of the fibre expresses dysferlin and behaves like A/W controls, whereas the other part is dysferlin-null and behaves like untransfected A/J fibres, losing amplitude and generating Ca^{2+} waves after OSI (Figs. 3 and 8). Thus, the leak of Ca^{2+} during and after injury that promotes broader Ca^{2+} dysregulation is likely to be localized and not widespread through the myoplasm. Future studies should reveal more details on the dynamics of Ca^{2+} waves in A/J myofibres.

Increased Ca^{2+} leak through the RyR1, which is likely to be induced by osmotic shock of dysferlin-null fibres, is thought to contribute to pathology in several forms of muscular dystrophy caused by mutations in the dystrophin–glycoprotein complex and other myopathies (Bellinger *et al.* 2009; Andersson *et al.* 2012). The pathways that lead from increased Ca^{2+} leak to pathogenesis in dysferlinopathies remain unknown, although, as in other myopathies, they may involve chemical modification of RyR1, calcium-induced proteolysis, mitochondrial dysfunction or ER stress (e.g. Ikezoe *et al.* 2003; Kobayashi *et al.* 2010; Andersson *et al.* 2012; Moorwood & Barton, 2014; Timpani *et al.* 2015). Ca^{2+}-induced proteolysis by calpain 3 is an attractive possibility, as it has been shown to occur in *mdx* myofibres and to be associated with degradation of junctophilin (Murphy *et al.* 2013), another triadic protein. Calpain 3 associates with and degrades dysferlin and the RyR1 (Huang *et al.* 2008; Kramerova *et al.* 2008; Lek *et al.* 2013; Redpath *et al.* 2014), however, making dissecting its contributions to the loss of the Ca^{2+} transient in injured dysferlin-null muscles a challenging task. Still, as 50 μM calpeptin did not protect A/J muscle fibres against the loss of the Ca^{2+} transient caused by OSI, calpains are unlikely to contribute. Furthermore, proteolysis of junctophilin does not appear to occur to a significant

extent in A/J muscle, suggesting that it is not associated with the differences in the Ca^{2+} transients seen in A/J and control myofibres. Our future studies will examine the relationship of these and other possible mechanisms to the pathophysiology of single dysferlin-null muscle fibres that we have described here.

In conclusion, our current findings provide new observations that link the pathogenesis seen in dysferlinopathies to changes in Ca^{2+} regulation. The exact mechanisms by which dysferlin helps to regulate Ca^{2+} homeostasis and excitation–contraction coupling in skeletal muscle will require further study, however. We also note that the drugs we have examined here have the potential to benefit individuals with dysferlinopathies by reducing the frequency of Ca^{2+} leak and related pathological changes in skeletal muscle.

References

Aksentsev SL, Rakovich AA, Okoon IM, Konev SV, Orlov SN & Kravtsov GM (1983). Effect of tetracaine on veratrine-mediated influx of sodium into rat brain synaptosomes. *Pflugers Arch* **397**, 135–140.

Andersson DC, Betzenhauser MJ, Reiken S, Meli AC, Umanskaya A, Xie W, Shiomi T, Zalk R, Lacampagne A & Marks AR (2011). Ryanodine receptor oxidation causes intracellular calcium leak and muscle weakness in aging. *Cell Metab* **14**, 196–207.

Andersson DC, Meli AC, Reiken S, Betzenhauser MJ, Umanskaya A, Shiomi T, D'Armiento J & Marks AR (2012). Leaky ryanodine receptors in β-sarcoglycan deficient mice: a potential common defect in muscular dystrophy. *Skelet Muscle* **2**, 9.

Bannister RA (2016). Bridging the myoplasmic gap II: more recent advances in skeletal muscle excitation-contraction coupling. *J Exp Biol* **219**, 175–182.

Bansal D & Campbell KP (2004). Dysferlin and the plasma membrane repair in muscular dystrophy. *Trends Cell Biol* **14**, 206–213.

Bansal D, Miyake K, Vogel SS, Groh S, Chen C-C, Williamson R, McNeil PL & Campbell KP (2003). Defective membrane repair in dysferlin-deficient muscular dystrophy. *Nature* **423**, 168–172.

Bellinger AM, Reiken S, Carlson C, Mongillo M, Liu X, Rothman L, Matecki S, Lacampagne A & Marks AR (2009). Hypernitrosylated ryanodine receptor calcium release channels are leaky in dystrophic muscle. *Nature Med* **15**, 325–330.

Böhle T (1992). The effect of the benzothiazepine diltiazem on force and Ca^{2+} current in isolated frog skeletal muscle fibres. *J Physiol* **445**, 303–318.

Braü ME, Vogel W & Hempelmann G (1998). Fundamental properties of local anesthetics: half-maximal blocking concentrations for tonic block of Na^+ and K^+ channels in peripheral nerve. *Anesth Analg* **87**, 885–889.

Brown LE, Clare JJ & Wray D (2009). Functional and pharmacological properties of human and rat NaV1.8 channels. *Neuropharmacology* **56**, 905–914.

Brum G, Piriz N, DeArmas R, Rios E, Stern M & Pizarro G (2003). Differential effects of voltage-dependent inactivation and local anesthetics on kinetic phases of Ca^{2+} release in frog skeletal muscle. *Biophys J* **85**, 245–254.

Burr AR & Molkentin JD (2015). Genetic evidence in the mouse solidifies the calcium hypothesis of myofiber death in muscular dystrophy. *Cell Death Differ* **22**, 1402–1412.

Caballero R, Gomez R, Nunez L, Moreno I, Tamargo J & Delpon E (2004). Diltiazem inhibits hKv1.5 and Kv4.3 currents at therapeutic concentrations. *Cardiovasc Res* **64**, 457–466.

Covian-Nares JF, Koushik SV, Puhl HL 3rd & Vogel SS (2010). Membrane wounding triggers ATP release and dysferlin-mediated intercellular calcium signaling. *J Cell Sci* **123**, 1884–1893.

Cully TR & Launikonis BS (2016). Leaky ryanodine receptors delay the activation of store overload-induced Ca^{2+} release, a mechanism underlying malignant hyperthermia-like events in dystrophic muscle. *Am J Physiol Cell Physiol* **310**, C673–C680.

Defour A, Van der Meulen JH, Bhat R, Bigot A, Bashir R, Nagaraju K & Jaiswal JK (2014). Dysferlin regulates cell membrane repair by facilitating injury-triggered acid sphingomyelinase secretion. *Cell Death Dis* **26**, e1306.

Demonbreun AR, Quattrocelli M, Barefield DY, Allen MV, Swanson KE & McNally EM (2016). An actin-dependent annexin complex mediates plasma membrane repair in muscle. *J Cell Biol* **213**, 705–718.

DiFranco M, Neco P, Capote J, Meera P & Vergara JL (2006). Quantitative evaluation of mammalian skeletal muscle as a heterologous protein expression system. *Prot Expr Purif* **47**, 281–288.

DiFranco M, Tran P, Quinonez M & Vergara J (2011). Functional expression of transgenic 1sDHPR channels in adult mammalian skeletal muscle fibres. *J Physiol* **589**, 1421–1442.

Dirksen RT & Avila G (2004). Distinct effects on Ca^{2+} handling caused by malignant hyperthermia and central core disease mutations in RyR1. *Biophys J* **87**, 3193–3204.

Döring F, Degtiar VE, Grabner M, Striessnig J, Hering S & Glossmann H (1996). Transfer of L-type calcium channel IVS6 segment increases phenylalkylamine sensitivity of α_{1A}. *J Biol Chem* **271**, 11745–11749.

Endo M (2009). Calcium-induced calcium release in skeletal muscle. *Physiol Rev* **89**, 1153–1176.

Evesson FJ, Peat RA, Lek A, Brilot F, Lo HP, Dale RC, Parton RG, North KN & Cooper ST (2010). Reduced plasma membrane expression of dysferlin mutants is attributed to accelerated endocytosis via a syntaxin-4-associated pathway. *J Biol Chem* **285**, 28529–28539.

Farini A, Sitzia C, Navarro C, D'Antona G, Belicchi M, Parolini D, Del Fraro G, Razini P, Bottinelli R, Meregalli M & Torrente Y (2012). Absence of T and B lymphocytes modulates dystrophic features in dysferlin deficient animal model. *Exp Cell Res* **318**, 1160–1174.

Ferry DR & Glossmann H (2016). Identification of putative calcium channels in skeletal muscle microsomes. *FEBS Lett* **148**, 331–337.

Fruen BR, Mickelson JR & Louis CF (1997). Dantrolene inhibition of sarcoplasmic reticulum Ca^{2+} release by direct and specific action at skeletal muscle ryanodine receptors. *J Biol Chem* **272**, 26965–26971.

Glover L & Brown RH Jr (2007). Dysferlin in membrane trafficking and patch repair. *Traffic* **8**, 785–794.

Goll A, Ferry DR & Glossmann H (1983). Target size analysis of skeletal muscle Ca^{2+} channels. Positive allosteric heterotropic regulation by d-cis-diltiazem is associated with apparent channel oligomer dissociation. *FEBS Lett* **157**, 63–69.

Gonzalez-Serratos H, Valle-Aquilera R, Lathrop DA & Garcia MC (1982). Slow inward calcium currents have no obvious role in muscle excitation-contraction coupling. *Nature* **298**, 292–294.

Han WQ, Xia M, Xu M, Boini KM, Ritter JK, Li NJ & Li PL (2012). Lysosome fusion to the cell membrane is mediated by the dysferlin C2A domain in coronary arterial endothelial cells. *J Cell Sci* **125**, 1225–1234.

Hering S, Aczél S, Grabner M, Döring F, Berjukow S, Mitterdorfer J, Sinnegger MJ, Striessnig J, Degtiar VE, Wang Z & Glossmann H (1996). Transfer of high sensitivity for benzothiazepines from L-type to class A (BI) calcium channels. *J Biol Chem* **271**, 24471–24475.

Hernandez-Deviez DJ, Howes MT, Laval SH, Bushby K, Hancock JF & Parton RG (2008). Caveolin regulates endocytosis of the muscle repair protein, dysferlin. *J Biol Chem* **283**, 6476–6488.

Ho M, Post CM, Donahue LR, Lidov HG, Bronson RT, Goolsby H, Watkins SC, Cox GA & Brown RH Jr (2004). Disruption of muscle membrane and phenotype divergence in two novel mouse models of dysferlin deficiency. *Hum Mol Gen* **13**, 1999–2010.

Hockerman GH, Dilmac N, Scheuer T & Catterall WA (2000). Molecular determinants of diltiazem block in domains IIIS6 and IVS6 of L-type Ca^{2+} channels. *Mol Pharmacol* **58**, 1264–1270.

Hockerman GH, Johnson BD, Abbott MR, Scheuer T & Catterall WA (1997). Molecular determinants of high affinity phenylalkylamine block of L-type calcium channels in transmembrane segment IIIS6 and the pore region of the α_1 subunit. *J Biol Chem* **272**, 18759–18765.

Huang Y, de Morree A, van Remoortere A, Bushby K, Frants RR, Dunnen JT & van der Maarel SM (2008). Calpain 3 is a modulator of the dysferlin protein complex in skeletal muscle. *Hum Mol Gen* **17**, 1855–1866.

Ikezoe K, Furuya H, Ohyagi Y, Osoegawa M, Nishino I, Nonaka I & Kira J (2003). Dysferlin expression in tubular aggregates: their possible relationship to endoplasmic reticulum stress. *Acta Neuropathol* **105**, 603–609.

Jiang D, Chen W, Xiao J, Wang R, Kong H, Jones PP, Zhang L, Fruen B & Chen SR (2008). Reduced threshold for luminal Ca^{2+} activation of RyR1 underlies a causal mechanism of porcine malignant hyperthermia. *J Biol Chem* **283**, 20813–20820.

Kerr JP, Ward CW & Bloch RJ (2014). Dysferlin at transverse tubules regulates Ca^{2+} homeostasis in skeletal muscle. *Front Physiol* **5**, 89.

Kerr JP, Ziman AP, Mueller AL, Muriel JM, Kleinhans-Welte E, Gumerson JD, Vogel SS, Ward CW, Roche JA & Bloch RJ (2013). Dysferlin stabilizes stress-induced Ca^{2+} signaling in the transverse tubule membrane. *Proc Natl Acad Sci USA* **110**, 20831–20836.

Kobayashi K, Izawa T, Kuwamura M & Yamate J (2010). The distribution and characterization of skeletal muscle lesions in dysferlin-deficient SJL and A/J mice. *Exp Toxicol Pathol* **62**, 509–517.

Kong H, Wang R, Chen W, Zhang L, Chen K, Shimoni Y, Duff HJ & Chen SR (2007). Skeletal and cardiac ryanodine receptors exhibit different responses to Ca^{2+} overload and luminal Ca^{2+}. *Biophys J* **92**, 2757–2770.

Kramerova I, Kudryashova E, Wu B, Ottenheijm C, Granzier H & Spencer MJ (2008). Novel role of calpain-3 in the triad-associated protein complex regulating calcium release in skeletal muscle. *Hum Mol Genet* **17**, 3271–3280.

Lamb GD (1986). Components of charge movement in rabbit skeletal muscle: the effect of tetracaine and nifedipine. *J Physiol* **376**, 85–100.

Lanner JT, Georgiou DK, Joshi AD & Hamilton SL (2010). Ryanodine receptors: structure, expression, molecular details, and function in calcium release. *Cold Spring Harb Perspec Biol* **2**, a003996.

Lek A, Evesson FJ, Lemckert FA, Redpath GM, Lueders AK, Turnbull L, Whitchurch CB, North KN & Cooper ST (2013). Calpains, cleaved mini-dysferlinC72, and L-type channels underpin calcium-dependent muscle membrane repair. *J Neurosci* **33**, 5085–5094.

Liewluck T, Pongpakdee S, Witoonpanich R, Sangruchi T, Pho-Lam T, Limwongse C, Thongnoppakhun W, Boonyapisit K, Sopassathit V, Phudhichareonrat S, Suthiponpaisan U, Raksadawan N, Goto K, Hayashi YK & Nishino I (2009). Novel DYSF mutations in Thai patients with distal myopathy. *Clin Neurol Neurosurg* **111**, 613–618.

Liu J, Aoki M, Illa I, Wu C, Fardeau M, Angelini C, Serrano C, Urtizberea JA, Hentati F, Hamida MB, Bohlega S, Culper EJ, Amato AA, Bossie K, Oeltjen J, Bejaoui K, McKenna-Yasek D, Hosler BA, Schurr E, Arahata K, de Jong PJ & Brown RH Jr (1998). Dysferlin, a novel skeletal muscle gene, is mutated in Miyoshi myopathy and limb girdle muscular dystrophy. *Nat Genet* **20**, 31–36.

Lukyanenko V & Györke S (1999). Ca^{2+} sparks and Ca^{2+} waves in saponin-permeabilized rat ventricular myocytes. *J Physiol* **521**, 575–585.

Mariano A, Henning A & Han R (2013). Dysferlin-deficient muscular dystrophy and innate immune activation. *FEBS J* **280**, 4165–4176.

McDade JR, Archambeau A & Michele DE (2014). Rapid actin-cytoskeleton-dependent recruitment of plasma membrane-derived dysferlin at wounds is critical for muscle membrane repair. *FASEB J* **28**, 3660–3670.

McNally EM, Ly CT, Rosenmann H, Mitrani Rosenbaum S, Jiang W, Anderson LV, Soffer D & Argov Z (2000). Splicing mutation in dysferlin produces limb-girdle muscular dystrophy with inflammation. *Am J Med Genet* **91**, 305–312.

McNeil PL, Miyake K & Vogel SS (2003). The endomembrane requirement for cell surface repair. *Proc Natl Acad Sci USA* **100**, 4592–4597.

Millay DP, Maillet M, Roche JA, Sargent MA, McNally EM, Bloch RJ & Molkentin JD (2009). Genetic manipulation of dysferlin expression in skeletal muscle: novel insights into muscular dystrophy. *Am J Pathol* **175**, 1817–1823.

Moorwood C & Barton ER (2014). Caspase-12 ablation preserves muscle function in the mdx mouse. *Hum Mol Genet* **23**, 5325–5341.

Murphy RM, Dutka TL, Horvath D, Bell JR, Delbridge LM & Lamb GD (2013). Ca^{2+}-dependent proteolysis of junctophilin-1 and junctophilin-2 in skeletal and cardiac muscle. *J Physiol* **591**, 719–729.

Nagaraju K, Rawat R, Veszelovsky E, Thapliyal R, Kesari A, Sparks S, Raben N, Plotz P & Hoffman EP (2008). Dysferlin deficiency enhances monocyte phagocytosis: a model for the inflammatory onset of limb-girdle muscular dystrophy 2B. *Am J Pathol* **172**, 774–785.

Nigro V & Savarese M (2014). Genetic basis of limb-girdle muscular dystrophies: the 2014 update. *Acta Myol* **33**, 1–12.

Nishikawa A, Mon-Yoshimura M, Segawa K, Hayashi YK, Takahashi T, Saito Y, Nonaka I, Krahn M, Levy N, Shimizu J, Mitsui J, Kimura E, Goto J, Yonemoto N, Aoki M, Nishino I, Oya Y & Murata M (2016). Respiratory and cardiac function in japanese patients with dysferlinopathy. *Muscle Nerve* **53**, 394–401.

Oulhen N, Onorato TM, Ramos I & Wessel GM (2014). Dysferlin is essential for endocytosis in the sea star oocyte. *Dev Biol* **388**, 94–102.

Peterson BZ, Johnson BD, Hockerman GH, Acheson M, Scheuer T & Catterall WA (1997). Analysis of the dihydropyridine receptor site of L-type calcium channels by alanine-scanning mutagenesis. *J Biol Chem* **272**, 18752–18758.

Pickering JD, White E, Duke AM & Steele DS (2009). DHPR activation underlies SR Ca^{2+} release induced by osmotic stress in isolated rat skeletal muscle fibers. *J Gen Physiol* **133**, 511–524.

Rawat R, Cohen TV, Ampong B, Francia D, Henriques-Pons A, Hoffman EP & Nagaraju K (2010). Inflammasome up-regulation and activation in dysferlin-deficient skeletal muscle. *Am J Pathol* **176**, 2891–2900.

Redpath GM, Woolger N, Piper AK, Lemckert FA, Lek A, Greer PA, North KN & Cooper ST (2014). Calpain cleavage within dysferlin exon 40a releases a synaptotagmin-like module for membrane repair. *Mol Biol Cell* **25**, 3037–3048.

Rios E, Figueroa L, Manno C, Kraeva N & Riazi S (2015). The couplonopathies: A comparative approach to a class of diseases of skeletal and cardiac muscle. *J Gen Physiol* **145**, 459–474.

Roche JA, Lovering RM & Bloch RJ (2008). Impaired recovery of dysferlin-null skeletal muscle after contraction-induced injury in vivo. *NeuroReport* **19**, 1579–1584.

Roche JA, Lovering RM, Roche R, Ru L, Reed PW & Bloch RJ (2010). Extensive mononuclear infiltration and myogenesis characterize the recovery of dysferlin-null skeletal muscle from contraction-induced injuries. *Am J Physiol Cell Physiol* **298**, C298–C312.

Roche JA, Ru LW, O'Neill AM, Resneck WG, Lovering RM & Bloch RJ (2011). Unmasking potential intracellular roles for dysferlin through improved immunolabeling methods. *J Histochem Cytochem* **59**, 964–975.

Roche JA, Tulapurkar ME, Mueller AL, van Rooijen N, Hasday JD, Lovering RM & Bloch RJ (2015). Myofiber damage precedes macrophage infiltration after in vivo injury in dysferlin-deficient A/J mouse skeletal muscle. *Am J Pathol* **185**, 1686–1698.

Shirokova N, Garcia J & Rios E (1998). Local calcium release in mammalian skeletal muscle. *J Physiol* **512**, 377–384.

Takagi A, Kojima S, Ida M & Araki M (1992). Increased leakage of calcium ion from the sarcoplasmic reticulum of the mdx mouse. *J Neurol Sci* **110**, 160–164.

Takahashi T, Aoki M, Suzuki N, Tateyama M, Yaginuma C, Sato H, Hayasaka M, Sugawara H, Ito M, Abe-Kondo E, Shimakura N, Ibi T, Kuru S, Wakayama T, Sobue G, Fujii N, Saito T, Matsumurua T, Funakawa I, Mukai E, Kawanami T, Morita M, Yamazaki M, Haegawa T, Shimizu J, Tsuji S, Kuzuhara S, Tanaka H, Yoshioka M, Konno H, Onodera H & Itoyama Y (2013). Clinical features and a mutation with late onset of limb girdle muscular dystrophy 2B. *J Neurol Neurosurg Psychiatry* **84**, 433–440.

Tamkun MM, Talvenheimo JA & Catterall WA (1984). The sodium channel from rat brain. Reconstitution of neurotoxin-activated ion flux and scorpion toxin binding from purified components. *J Biol Chem* **259**, 1676–1688.

Timpani CA, Hayes A & Rybalka E (2015). Revisiting the dystrophin-ATP connection: How half a century of research still implicates mitochondrial dysfunction in Duchenne Muscular Dystrophy aetiology. *Med Hypotheses* **85**, 1021–1033.

Tong J, McCarthy TV & MacLennan DH (1999). Measurement of resting cytosolic Ca^{2+} concentrations and Ca^{2+} store size in HEK-293 cells transfected with malignant hyperthermia or central core disease mutant Ca^{2+} release channels. *J Biol Chem* **274**, 693–702.

Uaesoontrachoon K, Cha HJ, Ampong B, Sali A, Vandermeulen J, Wei B, Creeden B, Huynh T, Quinn J, Tatem K, Rayavarapu S, Hoffman EP & Nagaraju K (2013). The effects of MyD88 deficiency on disease phenotype in dysferlin-deficient A/J mice: role of endogenous TLR ligands. *J Pathol* **231**, 199–209.

Urao N, Mirza RE, Heydemann A, Garcia J & Koh TJ (2016). Thrombospondin-1 levels correlate with macrophage activity and disease progression in dysferlin deficient mice. *Neuromuscul Disord* **26**, 240–251.

Vissing J (2016). Limb girdle muscular dystrophies: classification, clinical spectrum and emerging therapies. *Curr Opin Neurol* **29**, 635–641.

Wakizaka M, Eshima H, Tanaka Y, Shirakawa H, Poole DC & Kano Y (2017). In vivo Ca^{2+} dynamics induced by Ca^{2+} injection in individual rat skeletal muscle fibers. *Physiol Rep* **5**, e13180.

Walsh KB, Bryant SH & Schwartz A (1986). Effect of calcium antagonist drugs on calcium currents in mammalian skeletal muscle fibers. *J Pharmacol Exp Ther* **236**, 403–407.

Wang ZM, Messi ML & Delbono O (2002). Sustained overexpression of IGF-1 prevents age-dependent decrease in charge movement and intracellular Ca^{2+} in mouse skeletal muscle. *Biophys J* **82**, 1338–1344.

Williams JH (1990). Effects of low calcium and calcium antagonists on skeletal muscle staircase and fatigue. *Muscle Nerve* **13**, 1118–1124.

Yang T, Esteve E, Pessah IN, Molinski TF, Allen PD & López JR (2007). Elevated resting $[Ca^{2+}]_i$ in myotubes expressing malignant hyperthermia RyR1 cDNAs is partially restored by modulation of passive calcium leak from the SR. *Am J Physiol Cell Physiol* **292**, C1591–C1598.

Yin X, Wang Q, Chen T, Niu J, Ban R, Liu J, Mao Y & Pu C (2015). CD4+ cells, macrophages, MHC-I and C5b-9 involve the pathogenesis of dysferlinopathy. *Int J Clin Exp Pathol* **8**, 3069–3075.

Zholos A (2010). Pharmacology of transient receptor potential melastatin channels in the vasculature. *Br J Pharmacol* **159**, 1559–1571.

Additional information

Competing interests

There are no competing interests.

Author contributions

All experiments were performed in the Department of Physiology, University of Maryland School of Medicine. V.L. carried out experiments and prepared the figures. J.M.M. prepared the Venus-dysferlin construct, electroporated muscles, and cultured dissociated muscle fibres. V.L. and R.J.B. together designed the studies and wrote the paper. All authors have read and approved the paper, and agree to be accountable for all aspects of the work it describes. All authors qualify for authorship, and all qualified for authorship are listed as authors.

Funding

This research was supported by grants from the Jain Foundation, the Kahlert Foundation, the NIH (RO1 AR 064268), and the Muscular Dystrophy Association (no. 218313) to R.J.B.

Acknowledgements

We thank Andrea O'Neill, Sankeerth Manne, Alyssa Collier, and Emily Kleinhans-Welte for technical assistance, and Drs Chris Ward and W. Jon Lederer for useful discussions and for comments on the manuscript.

Supporting information

The following supporting information is available in the online version of this article.

Video S1. Spontaneous Ca^{2+} wave in an injured A/J myofibre.